

- (22) Doi, M.; Edwards, S. F. *J. Chem. Soc., Faraday Trans. 2* 1978, 74, 1789, 1802, 1818.
 (23) Lin, Y.-H. *Macromolecules* 1984, 17, 2846.
 (24) Kremer, K.; Binder, K. *J. Chem. Phys.* 1984, 81, 6381.
 (25) Fleischer, G.; Straube, E. *Polymer* 1985, 26, 241 and references therein.
 (26) Schumacher, S. Diplomarbeit, Mainz, 1985, unpublished.
 (27) Yamakawa, H. "Modern Theory of Polymer Solutions"; Harper and Row: New York, 1971.
 (28) Allen, V. R.; Fox, Th. G. *J. Chem. Phys.* 1964, 41, 337.
 (29) Montfort, J.-P.; Marin, G.; Monge, Ph. *Macromolecules* 1984, 17, 1551.

Diffusion of Intramolecular Cross-Linked and Three-Arm-Star Branched Polystyrene Molecules in Different Matrices

Markus Antonietti and Hans Sillescu*

*Institut für Physikalische Chemie der Universität Mainz, D-6500 Mainz, West Germany.
 Received July 17, 1985*

ABSTRACT: Diffusion coefficients D of photolabeled nonlinear polystyrene (PS) molecules in different PS matrices have been measured by using a holographic grating technique. Intramolecular cross-linked PS molecules (microgels) were prepared by Friedel-Crafts cross-linking with *p*-dichloroxylylene in dilute solution in a molecular weight range $25\,000 \leq M_w \leq 160\,000$ with average number of monomers between cross-links $P_c = 10, 20, 30$, and 40. The D values of microgels in microgel matrices decrease as the degree of cross-linking and the size of diffusant microgels are increased. At 194°C , $D = 9.0 \times 10^{-14} \text{ cm}^2 \text{ s}^{-1}$ for $M_w = 160\,000$ and $P_c = 20$, as compared with $1.9 \times 10^{-12} \text{ cm}^2 \text{ s}^{-1}$ for the corresponding linear PS. D of microgels ($P_c = 20$) in linear matrices ($16\,400 \leq M'_w \leq 160\,000$) is proportional to M'_w^{-1} for $M'_w \leq 40\,000$. D of small microgels becomes constant for larger M'_w and approaches the limit of a microgel matrix. For large microgels, D is found to be approximately $\sim M'_w^{-3}$ for $M'_w \geq 40\,000$, but has a weaker M'_w dependence for large M'_w . For three-arm-star PS in a microgel matrix D is proportional to $\exp(-\alpha M_w)$ over a D range from 3×10^{-11} to $8.7 \times 10^{-14} \text{ cm}^2 \text{ s}^{-1}$ for arm lengths from 80 to 420 monomer units at 194°C . In PS chain and star matrices, increased D values are obtained for diffusant molecular weights $M_w \gtrsim 100\,000$. The results are discussed in relation with current theories of polymer diffusion.

Introduction

Our diffusion studies in bulk polystyrene (PS) aim at separating different contributions to polymer motion by varying the topological structure of diffusant and matrix molecules. We have isolated the reptation contribution by dissolving PS chains in networks,¹ and we have shown that reptation dominates chain motion in a matrix of long chains. Deviations found in short-chain matrices² have been attributed to "tube formation" in a certain range above the entanglement spacing M_e . No reptation should be possible for ring-shaped macromolecules. In a previous study³ we have found PS ring diffusion surprisingly rapid, except for one sample that was probably heterogeneous.⁴ A recent investigation⁵ of PS ring diffusion in blends with PS chains also yields relatively rapid motion of small rings, whereas large rings diffuse much more slowly. The authors conclude that a mechanism other than reptation or constraint release is required to account for the diffusion of rings.

Intramolecular cross-linking introduces further constraints upon chain mobility. We have recently shown¹ that Friedel-Crafts cross-linking with *p*-dichloroxylylene provides highly flexible cross-links which preserve the local mobility up to very high cross-link densities. Thus, molecular microgels have become available that can neither reptate nor entangle with their neighbors, as no interpenetration is possible. Since the large bulk size of the microgels precludes usual vacancy mechanisms, the only possibility left for diffusion is through cooperative motion. Microgel diffusion in blends with linear PS should reveal to what extent the interpenetration of large chains affects motional freedom. We have shown previously¹ that chains reptate with the same diffusion coefficient through highly cross-linked microgel and continuous networks. In a forthcoming neutron diffraction study the swelling of

microgels by interpenetrating chains will be determined quantitatively. However, the interpenetration of chains may have less influence upon microgel or ring diffusion than the effect of entanglements. Klein⁶ has estimated that for ring lengths up to about ten entanglement lengths a large fraction of rings may diffuse by reptative motion since they are "non-obstacle-enclosing" in the sense that only entanglements are counted as obstacles forming the tube of the reptation model. In the present paper, the questions of what is an entanglement and how it is related with cooperative motion and tube formation will be dealt with primarily from the point of view of an experimentalist who contributes new experimental data. Thus, we have varied the size and the cross-link density of the microgels and have measured self-diffusion coefficients as well as diffusion coefficients in blends with linear PS as a function of the chain length. Furthermore, we have measured self-diffusion coefficients as well as diffusion coefficients in blends with linear PS as a function of the chain length. Furthermore, we have measured diffusion coefficients of three-arm-star branched PS in chain, star, and microgel matrices in order to investigate the influence of cooperative motion, arm retraction, and tube renewal.

Experimental Section

1. Intramolecular Cross-Linked Polystyrene. Molecular microgels were prepared by Friedel-Crafts cross-linking of linear PS with *p*-dichloroxylylene in dilute dichloroethane solution, as described in ref 1. This Friedel-Crafts reaction was also applied in order to prepare loop-shaped PS molecules from PS chains carrying a chloromethylbenzene end group introduced in the termination step of the anionic polymerization. Although one cannot be sure whether this "backbiting" reaction occurs in a random manner, we have estimated the loop size from the random walk in a good solvent⁷ and have obtained⁸ the number- and weight-average ring sizes of 65 and 385 monomers, respectively,

Table I
Characterization of Intramolecular Cross-Linked Polystyrene

M_w^a	M_w/M_n^b	P_c	ϕ_{PS}
25 000	1.07	40	0.010
25 000	1.08	30	0.005
25 000	1.10	20	0.004
25 000	1.11	10	0.002
45 800	1.09	40	0.010
45 800	1.09	30	0.005
45 800	1.10	20	0.004
45 800	1.12	10	0.002
67 000	1.05	20	0.004
100 000	1.09	40	0.008
100 000	1.10	30	0.005
100 000	1.09	20	0.002
100 000	1.08	10	0.002
134 000	1.07	20	0.002
160 000	1.05	40	0.005
160 000	1.04	30	0.002
160 000	1.05	20	0.002
160 000	1.06	10	0.002

^a Before cross-linking; $M_w/M_n < 1.04$. ^b After cross-linking.

Table II
Characterization of Three-Arm-Star Branched Polystyrenes

$M_w(\text{arm})$	$M_w(\text{star})$	$M_w/M_n(\text{star})$
8 300	26 000	1.10
18 500	58 200	1.10
25 600	71 500	1.12
31 200	82 200	1.08
34 300	92 000	1.08
43 700	114 600	1.07
55 600	142 500	1.09

for a chain of 1000 monomers. These numbers should also apply to the rings produced in the first step of intramolecular cross-linking. In this case, one should expect relatively homogeneous microgel networks. However, we cannot yet exclude that much smaller rings are formed if they are sterically favored for some unknown reason. We know from preliminary viscosity and light-scattering measurements that the size of the microgels is reduced with respect to the corresponding linear random coil size in solution. However, a more detailed characterization must await further results including data from X-ray and neutron scattering. The characterization of the samples by GPC is listed in Table I. P_c is the average number of monomers between cross-links; ϕ_{PS} is the volume fraction of PS in the cross-linking reaction. The microgel molecular weights in Figure 2 are augmented by the weight of the cross-links⁹ and the effect of partial dimerization (indicated by the larger polydispersity for high cross-linking in Table I).

2. Three-Arm-Star Branched Polystyrene. The anionic polymerization performed in tetrahydrofuran (THF) was initiated at -78°C with cumenylpotassium and terminated after heating with methyltrichlorosilane or methyltrichlorogermane to -20°C . Under these conditions, the reaction was sufficiently rapid in order to complete the reaction within 10 min, though the last termination step leading to stars is sterically hindered. The three-arm stars were separated from a small amount of four-arm stars and linear PS by fractional precipitation with methanol from THF solution. In Table II, the characterization of the samples by GPC is given. M'_w is the apparent star molecular weight determined by using the calibration for linear PS. For large stars, the ratio $M'_w(\text{star})/3M_w(\text{arm})$ is close to the theoretical value of 0.88 obtained by Zimm and Kilb¹⁰ for the ratio of the intrinsic viscosities. Possibly, the theory¹⁰ is not strictly applicable to our two smallest star samples where we find $M'_w(\text{star}) \geq 3M_w(\text{arm})$. Some short tailing is visible in the GPC curves, indicating incomplete separation of linear PS. However, the overall polydispersity (see Table II) is sufficiently small for the purpose of investigating the M_w dependence of the star diffusion coefficients. Since the diffusion of linear PS is much faster than that of the stars, they only contribute to the short-time decay of the forced Rayleigh scattering

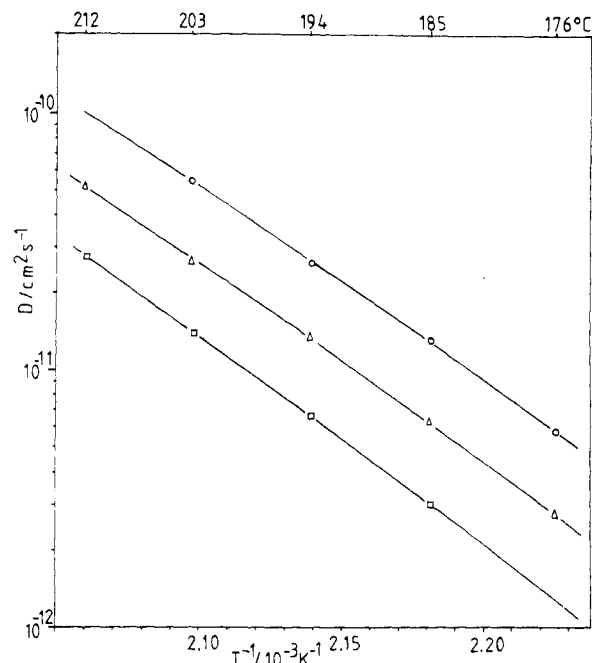


Figure 1. Diffusion coefficients of labeled linear and intramolecular cross-linked (microgel) polystyrene (PS): (circles) linear PS (weight-average degree of polymerization $P_w = 440$) in a long-chain matrix ($P'_w = 1000$); (triangles) microgel PS with $P_w = 440$ and $P_c = 40$ monomers between cross-links; (squares) microgel PS with $P_w = 440$ and $P_c = 10$.

curves and can readily be accounted for in the evaluation of the star diffusion coefficients. The thermal stability of the stars was tested by annealing the samples under vacuum for 5 days at 180°C . No thermal decay was observed in the subsequent GPC investigation.

3. Sample Preparation. The intracross-linked and three-arm-star branched PS molecules were labeled statistically at the phenyl groups by chloromethylation¹¹ and subsequent reaction with the Cs salt of 2-nitro-4-carboxy-4-(dimethylamino)stilbene.¹ For star molecules, it seems to be particularly important that the label concentration does not exceed an average of about 1 label per star molecule and that no chloromethyl groups remain. Distorted forced Rayleigh scattering decay curves and changed diffusion coefficients have been observed in some samples that did not meet these conditions. Pellets from mixtures of labeled and unlabeled PS were prepared, and the diffusion coefficient was measured by the holographic grating technique, as described previously.¹⁻³

Results and Discussion

1. Intramolecular Cross-Linked Polystyrene. Diffusion coefficients of photolabeled intramolecular cross-linked (microgel) PS are given in Figure 1 as a function of temperature for two different degrees of cross-linking. The D values of the corresponding linear PS in a long-chain matrix¹² are given for comparison. We first note that the very high cross-linking of the sample with $P_c = 10$ causes little change in the temperature dependence, indicating that the local mobility is essentially unaltered. The reduction of D by intramolecular cross-linking of PS chains is relatively small, in particular, if we realize that the reptation model applies to chain diffusion under these conditions ($D \sim P_n^{-2}$, see Figure 2 of ref 2). Perhaps, the 5–6 cross-linking molecules⁹ in a "microgel" having a weight-average degree of polymerization of $P_w = 440$ and $P_c = 40$ leave sufficient flexibility for relatively independent motion of individual particles. A higher cross-link density leads to less deformable microgels and an increased cooperativity of diffusive motion. This results in a large reduction of the D values as the size of the microgels is increased. A diffusion coefficient of 9.0×10^{-14}

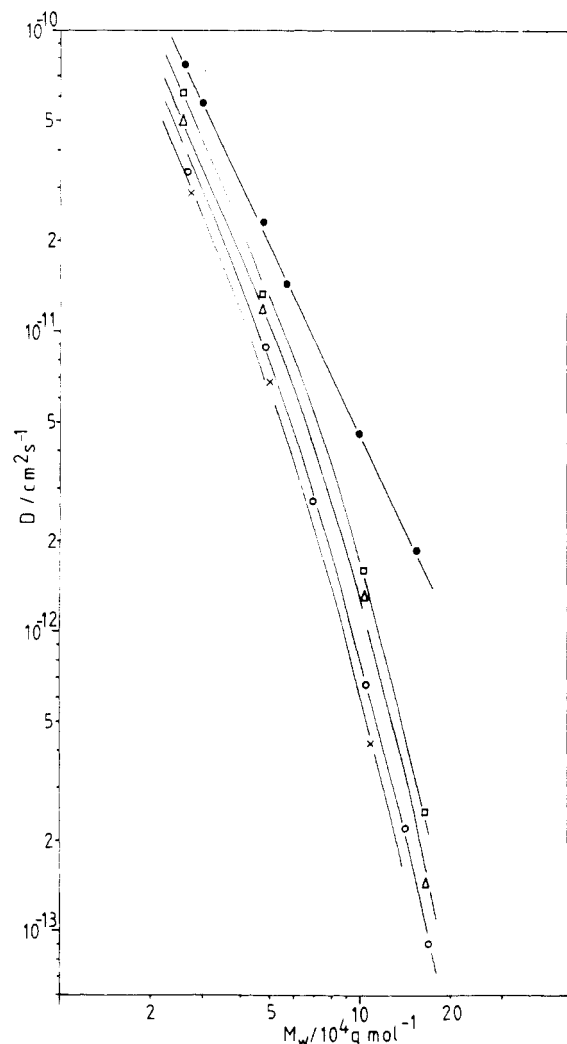


Figure 2. Diffusion coefficients of labeled microgel PS vs. their weight-average molecular weight M_w at 194 °C. The average number of monomers between cross-links is $P_c = 40, 30, 20$, and 10 for squares, triangles, circles, and crosses, respectively. Full circles are for labeled PS in a matrix of $P'_w = 1000$.

$\text{cm}^2 \text{s}^{-1}$ has been measured at 194 °C for a microgel with $P_w = 1540$ and $P_c = 20$, whereas the corresponding linear molecule has a D value of $1.9 \times 10^{-12} \text{ cm}^2 \text{s}^{-1}$; see Figure 2. It is difficult to estimate how many microgel particles of that size must cooperate in order to move one particle by its sphere size diameter of 8 nm. It is clear from Figure 2 that the dependence of D upon the cross-link density also increases with the microgel size. Of course, only deformable microgels can move at all in the dense medium of bulk PS. In order to relate some measure of deformability with the number of cooperatively moving particles a theory modeling diffusion in a dense system of deformable spheres would certainly be very helpful.

In Figure 3, the diffusion coefficients of labeled microgel molecules in matrices of linear PS measured at 194 °C are shown. The average chain length between cross-links was $P_c = 20$, the label concentration 1 label per 400 microgel monomers, and the microgel concentration in the matrix 12.5 wt %. This relatively high concentration allows for intermolecular interactions between the microgels which should be amplified by the possible swelling through interpenetrating chains, in particular, if long chains interpenetrate neighboring microgels. Three regimes of diffusive behavior can be detected in Figure 3. In short-chain matrices ($P'_w \lesssim 400$) the D values seem to be approximately proportional to P'_w^{-1} , although a somewhat weaker

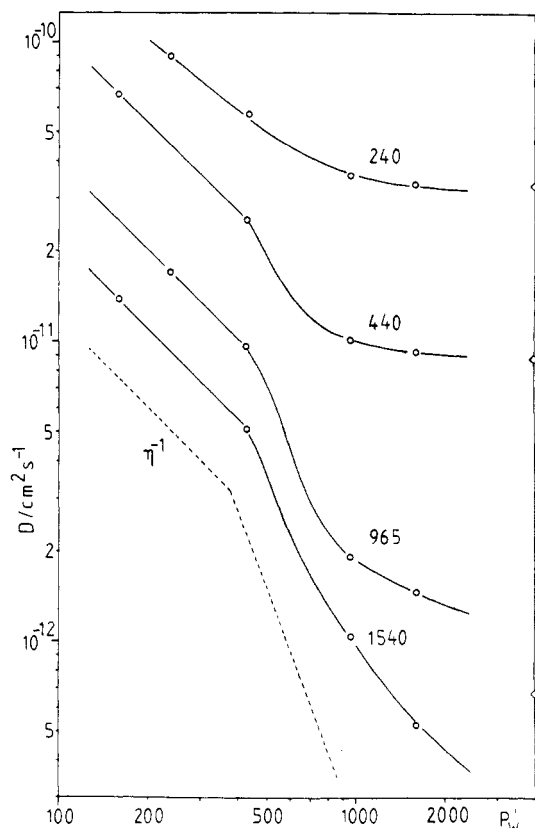


Figure 3. Diffusion coefficients of labeled microgel PS vs. P'_w of the matrix of linear PS at 194 °C. The numbers in the figure denote P_w of the microgels. The diamonds denote the D values in a microgel matrix (see Figure 2). The dashed line indicates the slopes of the inverse viscosity of the matrix.

dependence is also compatible with our data (Figure 3). For large microgels, a crossover to a second regime with a stronger P'_w dependence is observed which may approach the power law of the inverse viscosity ($\eta^{-1} \sim P'_w^{-3.4}$) indicated by the dashed line in Figure 3. One can discuss the idea that a large microgel molecule behaves like a sphere with the Stokes-Einstein diffusion coefficient $D = kT/6\pi\eta r_{\text{eff}}$, where η is the viscosity of the chain matrix and r_{eff} is some effective radius of the microgel. However, r_{eff} would become unreasonably large for large microgels, and the dependence of D upon the microgel molecular weight is much stronger than the $M^{-1/3}$ dependence expected for a bulk sphere. The two largest microgels scale approximately as M^{-1} for matrices $M' \lesssim 100\,000$. This is in accordance with the tube-renewal model^{6,7} which predicts $D \sim (M^{-1}M'^{-\beta})$, where $\beta = 2.5$ for entangled matrix chains if one takes into account⁶ that each tube-forming chain contributes a number ($\sim M'^{1/2}$) of constraints which are removed as the chain reptates away. Klein has argued⁶ that the tube-renewal mechanism should be ineffective for small "non-obstacle-enclosing" rings which contain no entanglements. Although a microgel can be considered as an assembly of small rings, it can enclose entanglements if its total size corresponds to that of a large ring. We can see from Figure 3 that large microgels detect the matrix crossover from nonentangled to entangled melts. This indicates that the total size of the diffusant determines whether entanglements are seen irrespective of the ring size. In contrast, it is apparent from the upper curve in Figure 3 that small microgels are not influenced by the entanglements of the matrix. For long chains, D becomes constant and approaches the value in the microgel matrix indicated by the diamond in Figure 3. For this microgel ($P_w = 240$), the diffusion coefficient has also been measured

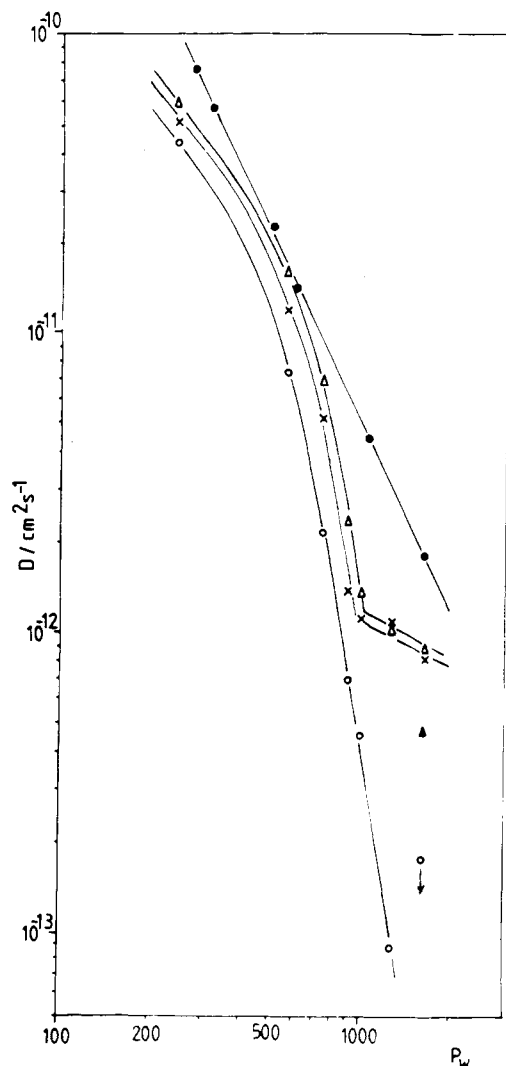


Figure 4. Diffusion coefficients of labeled three-arm-star PS vs. their weight-average degree of polymerization P_w at 194 °C: (triangles) matrix of linear PS with $P'_w = 1000$ (and $P'_w = 3330$ for full triangle); (crosses) matrix of three-arm-stars PS with $P'_w = 1605$; (circles) matrix of intramolecular cross-linked PS with $P'_w = 3330$ and $P_c = 33$. Full circles are for labeled linear PS in a matrix of $P'_w = 1000$.

in a linear matrix of longer chains ($P'_w = 3330$) and in a larger microgel matrix ($P'_w = 965$): almost the same asymptotic D value was found. This plateau behavior, which characterizes a *third regime* of diffusive motion, is also reached for the larger microgel of $P_w = 440$. Possibly, the D values of $6.6 \times 10^{-13} \text{ cm}^2 \text{ s}^{-1}$ and $0.90 \times 10^{-13} \text{ cm}^2 \text{ s}^{-1}$ measured for the microgels with $P_w = 965$ and 1540, respectively, in their microgel matrices are also limits to be attained asymptotically in matrices of very long chains. This result is rather puzzling since we feel sure that the chains interpenetrate the microgels (see Introduction). Now, the diffusion coefficients of long chains may be much smaller than those of the microgels interpenetrated by these chains. In a test experiment we have found that a labeled chain of $P_w = 1540$ has a D value of $1.3 \times 10^{-12} \text{ cm}^2 \text{ s}^{-1}$ in a microgel matrix of $P'_w = 440$ at 195 °C, whereas the microgel diffuses with $D = 8.8 \times 10^{-12} \text{ cm}^2 \text{ s}^{-1}$ in the same environment. Apparently the centers of mass of microgels and interpenetrating chains can move on different time scales if averaged over the long times ($>1 \text{ min}$) of our diffusion experiments. As an explanation, a result of recent simulations of chain dynamics in a tube confinement¹³ may be helpful. It was found that the mean square displacement $\langle [x_i(t) - x_i(0)]^2 \rangle$ of segment i along

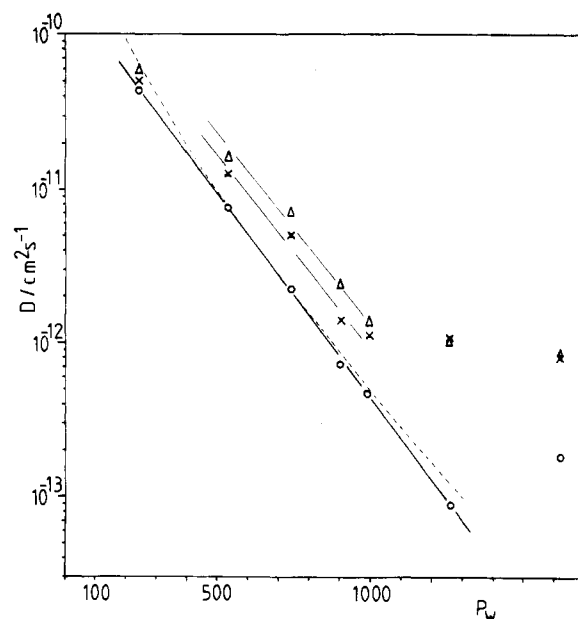


Figure 5. Semilogarithmic plot of the star diffusion coefficients of Figure 4. The symbols have the same meaning as in Figure 4.

the tube in the center of the mass system of the molecule increases as i is moved from the center to the ends of the chain. (See Figure 11 of ref 13.) Accordingly, it is conceivable that chain ends interpenetrate microgels on a time scale which is much faster than that of the center of mass, thus allowing for rapid microgel diffusion. As the density of the chain ends decreases with increasing chain length, the limiting D value in a matrix of vanishing chain end density should be close to D in a microgel matrix. It should be noted that the diffusion coefficient of small PS rings in a matrix of linear PS becomes also independent of the chain length for long chains.⁵

2. Three-Arm-Star Branched Polystyrene. The diffusion coefficients of three-arm-star PS in different matrices, measured at 194 °C, are shown in Figure 4. The average label concentration was 1 label per 800 star monomers, and the star concentration in the matrix was 20 wt %. The results in the microgel matrix (open circles in Figure 4) can be interpreted in terms of the theoretical prediction^{6,14-19}

$$D = D_0 N^{-\beta} \exp(-\alpha N) \quad (1)$$

where D_0 , α , and β are constants and N is proportional to the number of segments per arm. We choose $N = P_w$, the degree of polymerization of the total star molecule, in order to compare α and D_0 with the values determined by Klein for the diffusion of three-arm-star branched polyethylene (PE) in a linear PE matrix at 176 °C.¹⁸ The theoretical exponent β was obtained as $3^{14,15}$, 2^{16} , 1^{18} , 0.6^{19} and 0.5^{17} respectively, depending on the assumptions chosen for star diffusion in a network. In Figure 5, we compare a pure exponential fit ($\beta = 0$) with a fit for $\beta = 1$ (dashed line). Apparently, the exponential fit is better; however, we cannot rule out exponents $0 < \beta \leq 1$ in view of the experimental uncertainty, impurities in the star samples, and a possible label influence upon arm motion (see Experimental Section). It should be noted that the D value for the largest stars ($P_w = 1605$) is too large since the forced Rayleigh scattering decay curves showed an influence of convective motion.

The α values determined for PS are larger than those given by Klein for PE, whereas the D_0 values are smaller for PS than for PE, cf. Table III. Let us evaluate these

Table III
Comparison of Star Diffusion Coefficients with Theoretical Predictions

matrix	β	$\alpha/10^{-3}$	α_b	$D_0, \text{cm}^2 \text{s}^{-1} (c = 1)$	$D_0', \text{cm}^2 \text{s}^{-1}$	$D_0^{\text{lin}}, \text{cm}^2 \text{s}^{-1}$
microgel PS	0	6.3	3.3	2.4×10^{-10}		
	1	4.5	2.3	4.6×10^{-8}	3.8×10^{-11}	8.9×10^{-11}
linear PE	0	4.2	1.13	3.9×10^{-8}		
	1	2.8	0.76	8.2×10^{-6}	4.1×10^{-8}	5.3×10^{-7}

parameters further in terms of Klein's recent theoretical expressions for star motion in a fixed-obstacle lattice.^{18,6} Essentially, he combines star motion by arm retraction to the center with a further mechanism where the center moves down one of the arm tubes, dragging the other arms with it.

He obtains

$$D' = c\alpha_b N_b D'_{\text{rep}}(N_b) \exp(-\alpha_b N_b) \quad (2)$$

c is a constant of the order 1 or $\approx 12\alpha_b$ depending on how arm "retraction" and "dragging" are combined. N_b is the number of entanglement lengths per branch related by

$$N = P_w = 3P_e N_b \quad (3)$$

with the total degree of polymerization N and the entanglement spacing P_e . $D'_{\text{rep}}(N_b)$ is the reptative diffusion coefficient of a linear chain of N_b segments. By combining eq 1-3, we obtain

$$\alpha_b = 3P_e \alpha \quad (4)$$

$$D_0' = N_b^2 D'_{\text{rep}}(N_b) = D_0/9cP_e^2 \alpha \quad (5)$$

D_0' can be compared with the experimental expression

$$D_0^{\text{lin}} = N_b^2 D_{\text{lin}}(N_b) \quad (6)$$

where $D_{\text{lin}}(N_b)$ is the experimental diffusion coefficient of a linear chain in the same matrix. The results of this comparison are shown in Table III. We have chosen $P_e = 174$ for PS and 89.3 for PE.²⁰ D_0^{lin} was obtained from ref 1 for PS chains in a microgel network and from ref 18 for PE chains in a matrix of linear PE. For PS, the experimental D_0^{lin} is relatively close to D_0' if $c = 1$, whereas for PE the difference is much larger, which is also apparent in Figure 6 of ref 18 showing a more rapid chain vs. star diffusion as compared with our Figure 4 for PS. We have no explanation for the origin of this difference. The α_b values given in Table III are roughly of the order 1 as predicted by the theory.

The diffusion coefficients of PS stars in matrices of star and linear PS are generally larger than the corresponding values in the microgel matrix, cf. Figure 4. This difference is of the same order as the matrix effect for the diffusion of linear PS shown in Figure 4 of ref 1. For large stars, $P_w \gtrsim 1000$, the D values are above the exponential prediction of eq 1. A similar behavior has been found by Klein for large PE stars in a linear matrix and was attributed to tube-renewal effects.¹⁸ More experimental D values measured as a function of matrix chain or arm lengths are necessary before a quantitative comparison with expressions from tube-renewal models is possible.

Conclusions

The diffusion coefficients of labeled PS microgel molecules in matrices of the same microgels decrease on increasing the cross-link density. Although the size reduction by cross-linking leads to smaller diffusant particles, the reduced deformability causes slower diffusion since non-interpenetrating microgels can only move by a cooperative process. Our results (Figure 2) provide a measure of how much this cooperative motion contributes to diffusion in comparison with the reptative process dominant in linear-chain diffusion. The diffusion of microgels in matrices

of linear PS can be characterized by three regimes. In short-chain matrices, below the critical viscosity molecular weight, D is roughly proportional to P_w^{-1} , thus detecting the Rouse dynamics of the matrix. For matrices of larger entangled chains the D values of large microgels follow approximately the molecular weight dependence of the inverse viscosity, $D \sim P_w^{-3}$, but the P_w dependence becomes weaker for very long chains and possibly approaches the plateau behavior found for the diffusion of small microgels (Figure 3). The latter do not detect the entanglement coupling of the long matrix chains but approach a constant D value identical with that in a microgel matrix. Apparently, the centers of mass of small microgels and interpenetrating long chains can move independently on different time scales. An explanation can possibly be obtained from recent simulations of chain motion in a tube constraint.¹³ Here, the segment motion relative to the center of mass motion is larger for segments close to the ends as compared with segments close to the center of chain.

The diffusion of three-arm-star PS in a microgel matrix follows an exponential law over a D range of almost three decades, thus supporting de Gennes' arm-retraction mechanism.¹⁴ Different assumptions on arm and center motion lead to different exponents β of the preexponential molecular weight factor in eq 1. Within our experimental accuracy we can safely rule out exponents $\beta > 1$,¹⁴⁻¹⁶ whereas $\beta \leq 1$ ¹⁷⁻¹⁹ is still in accordance with our results. Diffusion of PS stars in matrices of star and linear PS deviates from the exponential law for large diffusant stars, $P_w \gtrsim 1000$. The deviations are caused by "tube-renewal" effects of the matrix, but more experimental data are required in order to perform a quantitative comparison with current tube-renewal models.

Acknowledgment. Support by the Deutsche Forschungsgemeinschaft (Sonderforschungsbereich 41) and the Fonds der Chemischen Industrie is gratefully acknowledged. We are grateful to J. Klein and E. J. Kramer for sending preprints of their recent work.

Registry No. PS (homopolymer), 9003-53-6; *p*-dichloroxylylene, 623-25-6.

References and Notes

- (1) Antonietti, M.; Sillescu, H. *Macromolecules* **1985**, *18*, 1162.
- (2) Antonietti, M.; Coutandin, J.; Sillescu, H. *Macromolecules*, preceding paper in this issue.
- (3) Antonietti, M.; Coutandin, J.; Grütter, R.; Sillescu, H. *Macromolecules* **1984**, *17*, 789.
- (4) No diffusion was observed in this sample obtained by evaporating a solution of fluorescein (FL) labeled PS rings and linear PS of $M_w = 110\,000$, and this was explained erroneously by formation of a network when the long chains thread through more than one ring. Afterward, we discovered segregation effects in blends of FL-labeled rings with shorter chains where the samples became turbid, depending upon chain length and temperature. Accordingly, we now attribute the peculiar results shown in Figure 7 of ref 3 to association effects related with the onset of segregation. No segregation effects were observed after changing from FL to labeling with 2-nitro-4-carboxy-4'-(dimethylamino)stilbene, cf. ref 8.
- (5) Mills, P. J.; Mayer, J. W.; Kramer, E. J.; Hadzioannou, G.; Lutz, P.; Strazielle, C.; Rempp, P.; Kovacs, A. Abstract submitted for the General Meeting of the American Physics Society, March 1985.
- (6) Klein, J. *Macromolecules*, in press.

- (7) de Gennes, P. G. "Scaling Concepts in Polymer Physics"; Cornell University Press, Ithaca, NY, 1979.
- (8) Antonietti, M. Dissertation, Mainz University, 1985.
- (9) It should be noted that P_c^{-1} is twice the number of $-\text{CH}_2\text{C}_6\text{H}_4\text{CH}_2-$ units per monomer. The same notation was used in ref 1.
- (10) Zimm, B. H.; Kilb, R. W. *J. Polym. Sci.* **1959**, *37*, 19.
- (11) Coutandin, J.; Sillescu, H.; Voelkel, R. *Makromol. Chem., Rapid Commun.* **1982**, *3*, 649.
- (12) Ehlich, D. Diplomarbeit, Mainz University, 1984.
- (13) Kremer, K.; Binder, K. *J. Chem. Phys.* **1984**, *81*, 6381.
- (14) de Gennes, P. G. *J. Phys.* **1975**, *36*, 1199.
- (15) Doi, M.; Kuzuu, N. Y. *J. Polym. Sci., Polym. Lett. Ed.* **1980**, *18*, 775.
- (16) Graessley, W. W. *Adv. Polym. Sci.* **1982**, *47*, 67.
- (17) Pearson, D. S.; Helfand, E. *Faraday Symp. Chem. Soc.* **1983**, *18*, 189.
- (18) Klein, J.; Fletcher, D.; Fetters, L. J. *Nature (London)* **1983**, *304*, 526. *Faraday Symp. Chem. Soc.* **1983**, *18*, 159.
- (19) Needs, R. J.; Edwards, S. F. *Macromolecules* **1983**, *16*, 1492.
- (20) Ferry, J. D. "Viscoelastic Properties of Polymers", 3rd ed.; Wiley: New York, 1980.

Real-Time Spectral Acquisition and Size Exclusion Chromatography Combined To Give Verification of Copolymerization and Analysis of Composition, All as a Function of Molecular Size

John J. Meister,* John C. Nicholson, Damodar R. Patil, and Larry R. Field

*Department of Chemistry, Southern Methodist University, Dallas, Texas 75275.
Received July 9, 1985*

ABSTRACT: A new size exclusion analysis method that uses real-time acquisition of UV as a means of detection has been developed for compositional analysis of copolymer as a function of molecular size. This procedure enables proof of copolymerization. This size exclusion technique depends on distinct ultraviolet absorbance spectra arising from 2 parts of a copolymer to resolve total ultraviolet absorbance of the copolymer into that due to each part. Upon calibration of the detector, copolymer composition plots as a function of molecular weight or molecular size can be made. Absolute percentage error in the method is $\pm 4\%$. However, this error can be larger with different solvents, different amounts of aggregation, and/or different polymer structures which affect the absorbance spectrum of either copolymer part. Wavelengths at which absorbance of the copolymer parts are monitored must be chosen to maximize the difference in molar absorptivity of the parts. The method has been used to prove graft copolymerization and investigate the composition variation with molecular size in poly(lignin-*g*-(1-amidoethylene-*co*-[1-(*N*-(4-methoxyphenyl)amido)ethylene])).

Introduction

Copolymers are a particularly difficult class of polymers to characterize. They are, as Hamielec describes them,¹ complex polymers having random, block, or graft distribution of their repeat units. Properties of a copolymer depend on molecular composition and internal structure. Composition exerts a major control on physical properties, yet the composition distribution curve, which is the mole fraction of one monomer in the molecule plotted vs. the total weight percent of the sample with that mole fraction or less of monomer, is usually broader than the molecular weight distribution.² For random and block copolymers, the composition may not correlate with molecular weight.³ The composition of graft copolymers generally correlates with molecular weight since the mole fraction of side chain can only increase by increasing molecular weight.

Under the label of internal structure effects, random or block copolymer structural characteristics such as sequence lengths and tacticity control product absorbance and light wavelength absorbed,⁴ while graft copolymer structure characteristics, such as number of grafts per backbone molecule and average graft length control molecular size and shape.⁵ Since several 1-phenylethylene copolymers have significant commercial importance, there have been extensive efforts to analyze these materials.⁶⁻¹¹ Methods used to analyze these and other copolymers include fractionation, thin-layer chromatography, light scattering, thermal analysis, infrared spectroscopy, and liquid chromatography. Liquid chromatography methods used are based on partition,¹² adsorption,¹³ and size exclusion.¹⁴ Size

exclusion chromatography is the method used here to analyze complex polymers.

Size exclusion chromatography (SEC) separates the solutes in a solution based on the size or hydrodynamic volume of the molecules. Sorting takes place by passing solution through a column containing a microporous packing. For simple, linear homopolymers, the apparatus and column can be calibrated to relate size, as measured by the volume of solvent eluted between injection and elution of the molecule, to molecular weight. This calibration is performed by measuring elution volume for a series of standards of known molecular weight and holds for the particular temperature and solvent of the calibration experiment.

For complex polymers such as copolymers, molecular size depends on several variables besides molecular weight. These other variables are molecular composition and molecular configuration.¹ Elution volume of a complex polymer is thus often given only as a function of molecular size. Other analyses on the copolymer are possible, however, and several research groups^{4,15,16} have studied the composition and configuration of copolymers by size exclusion techniques.

In the following sections, SEC will be used to (i) verify grafting in a graft copolymer, thus proving bonding between the two molecular components, (ii) analyze component distribution in a complex polymer as a function of size, and (iii) provide backbone or side-chain analyses of a copolymer sample as a function of molecular size. This method provides more definitive evidence of grafting than